Article

Molecular Cell

Deacetylation of Nuclear LC3 Drives Autophagy Initiation under Starvation

Graphical Abstract

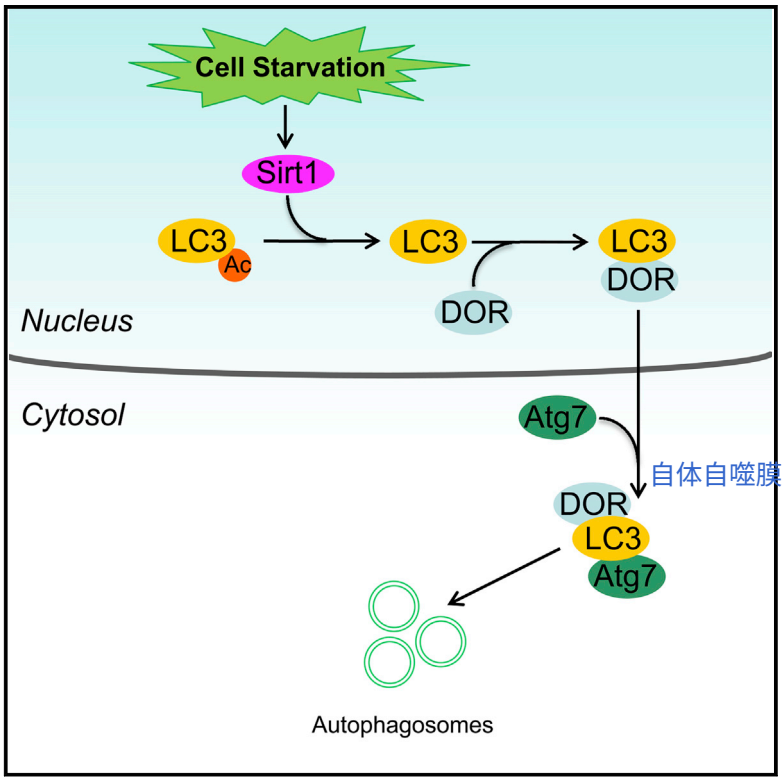

Authors

Rui Huang, Yinfeng Xu, ..., Jennifer Lippincott-Schwartz, Wei Liu

Correspondence

liuwei666@zju.edu.cn

In Brief

LC3 is a key autophagy regulator distributed abundantly in the nucleus. The regulation of nuclear LC3 redistribution to the cytoplasm and its coordination with LC3 conjugation to autophagic membranes is undefined. Huang et al. have identified an acetylation/deacetylation-dependent mechanism for the nucleocytoplasmic transport and activation of LC3 in starvation-induced autophagy.

Highlights

- Redistribution of nuclear LC3 to cytoplasm during cell starvation
- Nuclear LC3 is essential for starvation-induced autophagosome formation
- Sirt1 deacetylates LC3 at K49 and K51 in the nucleus
- Deacetylation of LC3 is required for LC3-Atg7 interaction

脱乙酰

Huang et al., 2015, Molecular Cell 57, 456–466
February 5, 2015
http://dx.doi.org/10.1016/j.molcel.2014.12.013

CellPress

Molecular Cell
Article

Deacetylation of Nuclear LC3 Drives Autophagy Initiation under Starvation

Rui Huang,[1] Yinfeng Xu,[1] Wei Wan,[1] Xin Shou,[1] Jiali Qian,[1] Zhiyuan You,[1] Bo Liu,[1] Chunmei Chang,[1] Tianhua Zhou,[1] Jennifer Lippincott-Schwartz,[2] and Wei Liu[1,3,*]

[1]Department of Biochemistry and Molecular Biology, Program in Molecular and Cell Biology, Zhejiang University School of Medicine, Hangzhou 310058, China

[2]Cell Biology and Metabolism Program, Eunice Kennedy Shriver National Institute of Child Health and Human Development, NIH, Bethesda, MD 20892, USA

[3]Collaborative Innovation Center for Diagnosis and Treatment of Infectious Disease, First Affiliated Hospital, Zhejiang University School of Medicine, Hangzhou 310003, China

*Correspondence: liuwei666@zju.edu.cn

http://dx.doi.org/10.1016/j.molcel.2014.12.013

SUMMARY

Shuttling of macromolecules between different cellular compartments helps regulate the timing and extent of different cellular activities. Here, we report that LC3, a key initiator of autophagy that cycles between the nucleus and cytoplasm, becomes selectively activated in the nucleus during starvation through deacetylation by the nuclear deacetylase Sirt1. Deacetylation of LC3 at K49 and K51 by Sirt1 allows LC3 to interact with the nuclear protein DOR and return to the cytoplasm with DOR, where it is able to bind Atg7 and other autophagy factors and undergo phosphatidylethanolamine conjugation to preautophagic membranes. The association of deacetylated LC3 with autophagic factors shifts LC3's distribution from the nucleus toward the cytoplasm. Thus, an acetylation-deacetylation cycle ensures that LC3 effectively redistributes in an activated form from nucleus to cytoplasm, where it plays a central role in autophagy to enable the cell to cope with the lack of external nutrients.

INTRODUCTION

Autophagy is a self-digestion process in which portions of the cytoplasm, including protein aggregates and damaged organelles, are encapsulated by double-membraned structures and delivered to lysosomes for degradation (Klionsky, 2007; Mizushima, 2007; Mizushima et al., 2010). All cells undergo basal levels of autophagy to maintain homeostasis, but starved cells upregulate autophagy significantly to enable recycling of nutrients. A key regulator of autophagy is LC3 (the microtubule-associated protein 1 light chain 3, a mammalian homolog of yeast Atg8), which controls major steps in the autophagic pathway including the growth of autophagic membranes, recognition of autophagic cargoes, and the fusion of autophagosomes with lysosomes (Ichimura et al., 2000; Nakatogawa et al., 2007; Noda et al., 2010; Pankiv et al., 2010). These functions of LC3 are built on an ubiquitination-like system by which soluble LC3 is converted to the membrane-bound form via conjugation with phosphatidylethanolamine (PE) with the assistance of the E1-like enzyme Atg7 and the E2-like enzyme Atg3 (Ichimura et al., 2000). Various signaling pathways are known to trigger autophagy during starvation (Kamada et al., 2000; Kim et al., 2011; Lin et al., 2012; Wei et al., 2013), but exactly what occurs mechanistically to enable LC3 to interact with Atg7 and other autophagy effectors to thereafter initiate autophagosome biogenesis is unclear.

In spite of functioning primarily in the cytoplasm where the autophagosomes and autolysosomes form, both endogenous and exogenous LC3 are abundant in the nucleus (Drake et al., 2010; Eskelinen, 2008; Guo et al., 2012; Mizushima et al., 2010; Waters et al., 2009). Kinetic analyses have indicated that instead of existing as a freely diffusing monomer, both cytoplasmic and nuclear LC3 is incorporated into a macromolecular complex (Drake et al., 2010; Kraft et al., 2014). Biochemical studies have also revealed that nuclear proteins constitute a significant group in the proteins identified in LC3-positive autophagosomes (Gao et al., 2010a; Mauvezin et al., 2010), suggesting that these nuclear proteins may be important components of the autophagic machinery involved in the inception or maturation of autophagosomes (Mauvezin et al., 2010; Nowak et al., 2009; Tang et al., 2010). It has been postulated that, in addition to functioning in autophagy, LC3 is involved in other cellular functions (Furuta et al., 2002; Zhou et al., 1997). Alternatively, nuclear LC3 may serve as a reserve for the cytoplasmic pool and shifts to the cytosol when soluble cytoplasmic LC3 is transformed to the lipidated type and incorporated into autophagic membranes (Drake et al., 2010; Hailey et al., 2010). Therefore, one puzzling issue about the nuclear LC3 is whether and how it participates in the formation of autophagosomes.

In this study, we have identified the essential role of the nuclear localization of LC3 in autophagosome formation. Before it can undergo large-scale conjugation to cytoplasmic membranes and initiate autophagy in response to starvation, nuclear LC3 redistributes out of the nucleus. This process is regulated by the nuclear deacetylase Sirt1, and deacetylations at K49 and K51 by Sirt1 coordinate the translocation with the membrane conjugation of LC3.

RESULTS

Nuclear Export of LC3 during Autophagy

We began by examining the subcellular localization of LC3 under fed and starved conditions using either endogenous

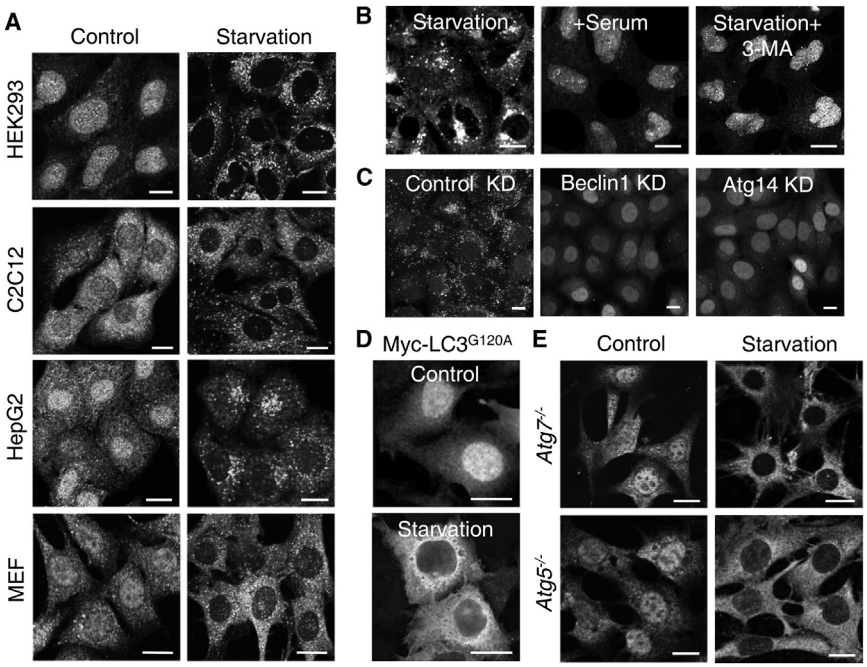

Figure 1. Nuclear Export of LC3 during Cell Starvation

(A) Redistribution of LC3 in starved cells. The cells were stained with specific LC3 antibody and visualized with confocal microscopy.

(B) Distribution of LC3 in starved HEK293 cells with or without 3-MA followed by readdition of serum for 2 hr.

(C) HeLa cells stably expressing GFP-LC3 were treated with either nontargeting siRNA or siRNAs for Beclin1 or Atg14 and were starved.

(D) Immunofluorescent images of starved HEK293 cells expressing Myc-LC3^{G120A}.

(E) Location of LC3 in starved *Atg7*$^{-/-}$ and *Atg5*$^{-/-}$ MEF cells.

All images were confocal images of optical slice thickness ~1 μm. Scale bars represent 10 μm. See also Figure S1.

(antibody) or exogenous (i.e., GFP-LC3) markers for LC3 in multiple cell lines. In all cases, LC3 in fed cells (i.e., control) showed typical nucleocytoplasmic localization with strong distribution in the nucleus (Figure 1A; Figure S1A available online). LC3 in starved cells, in contrast, resided primarily in the cytoplasm including cytoplasmic puncta indicative of autophagosomes (Figures 1A and S1A). The same phenomenon occurred with the other isoforms of Atg8 (Figure S1B). The starvation-induced redistribution of LC3 was reversible: within 2 hr of serum replenishment, cytoplasmic puncta containing LC3 largely disappeared and the protein reappeared in the nucleus (Figure 1B, +Serum). Therefore, LC3 only becomes concentrated in the cytoplasm, moving out of the nucleus, upon induction of autophagy.

LC3 undergoes constitutive slow cycling in and out of the nucleus (Drake et al., 2010). One possible mechanism for how LC3 shifts its distribution into the cytoplasm under starvation conditions is for the cycling pool of LC3 to become trapped in the cytoplasm by becoming associated with factors that prevent or retard it from cycling back into the nucleus. Supporting this possibility, we found less cytoplasmic redistribution of nuclear LC3 in cells starved in the presence of the phosphatidylinositol 3-kinase (PI3K)-III inhibitor 3-methyladenine (3-MA), and in starved Beclin1 or Atg14 knockdown cells, in which the early events in the assembly of autophagosomal factors on membranes were disrupted (Figures 1B, 1C, and S1C). Nonetheless, expression of the LC3 mutant Myc-LC3^{G120A}, which cannot conjugate with PE, in starved cells revealed the mutant protein still redistributed from nucleus to cytoplasm, even though it did not associate with cytoplasmic autophagic structures (Figure 1D). This suggested that LC3 redistribution into the cytoplasm during starvation does not require its conjugation to membranes. Furthermore, we found that LC3 redistribution into the cytoplasm in starved *Atg5*$^{-/-}$ or *Atg7*$^{-/-}$ cells, although no LC3 association with autophagic puncta occurred (Figure 1E). Therefore, LC3 redistribution into the cytoplasm, while dependent on autophagic signals, is not dependent on LC3 binding to membranes or on Atg5 or Atg7 activities.

Nuclear LC3 Is Essential for Starvation-Stimulated Autophagosome Formation

We next explored the function of nuclear localized LC3 and its relationship to the induction of autophagy in the cytoplasm. For this, we performed photobleaching or photoactivation experiments to selectively highlight nuclear or cytoplasmic pools of LC3 tagged with GFP or PAGFP. Upon selective highlighting of LC3's nuclear pool at starvation initiation, we observed visible LC3 molecules moving into the cytoplasm and associating with punctate structures (Figures 2A–2C). Therefore, nuclear-localized LC3 molecules actively redistribute from nucleus into cytoplasm onto autophagic puncta under starvation. Surprisingly, when we selectively highlighted the cytoplasmic pool of LC3 by photobleaching or photoactivating (Figures 2A and 2C, lower images), little, if any, of the highlighted molecules subsequently associated with autophagic puncta. This suggested that it is only the nuclear-localized pool of LC3 that has the ability to become conjugated to PE and bind to preautophagic membranes.

As a further test to this possibility, we expressed a LC3 construct containing a nuclear exit signal (NES-LC3) that does not accumulate in the nucleus in nutrient-rich cells. When these cells were nutrient depleted, LC3 failed to associate with autophagic membranes (Figure 2D). A possible obstruction in the formation of preautophagosomal structures in these cells was excluded by the normal generation of puncta with RFP-tagged double FYVE-containing protein 1 (RFP-DFCP1; Figure 2E), which associates with PI3P and is used as a marker of the omegasomes (Axe et al., 2008; Matsunaga et al., 2010). We further performed knockdown and rescue experiments to confirm the

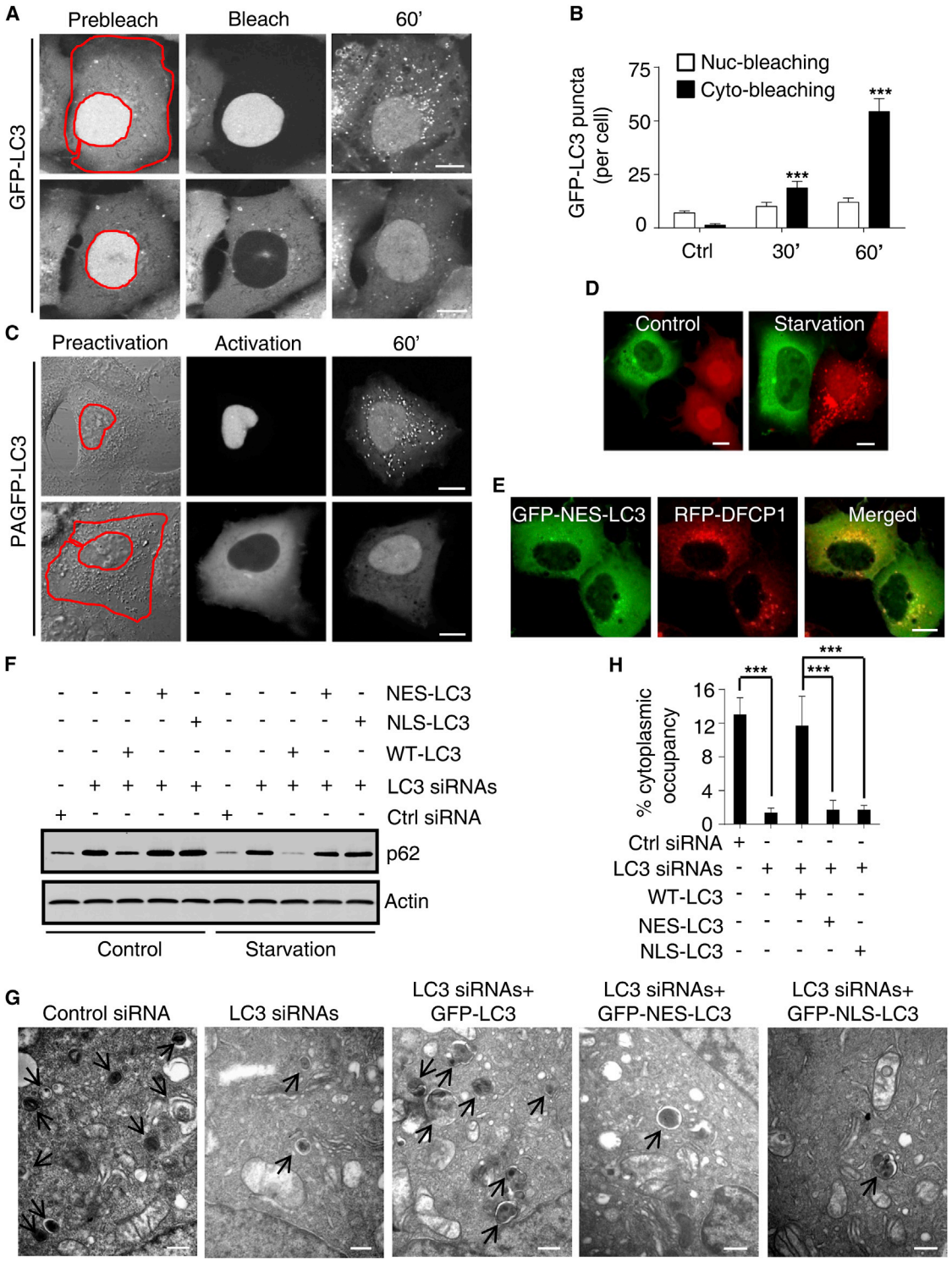

Figure 2. Nuclear LC3 Is Essential for Starvation-Stimulated Autophagosome Formation

(A) HEK293 cells stably expressing GFP-LC3 were imaged before and after photobleaching the cytosolic or nuclear pool (outlined in red) of GFP-LC3, followed by starvation. Note the formation of GFP-LC3 puncta in the cytoplasm.

(B) Quantification of GFP-LC3 puncta in 15 nuclear or cytoplasmic photobleached cells.

(C) HEK293 cells transiently expressing PAGFP-LC3 were imaged with low levels of 488 nm laser light before and after irradiation of the selected region (outlined in red) with 405 nm light, followed by starvation.

(legend continued on next page)

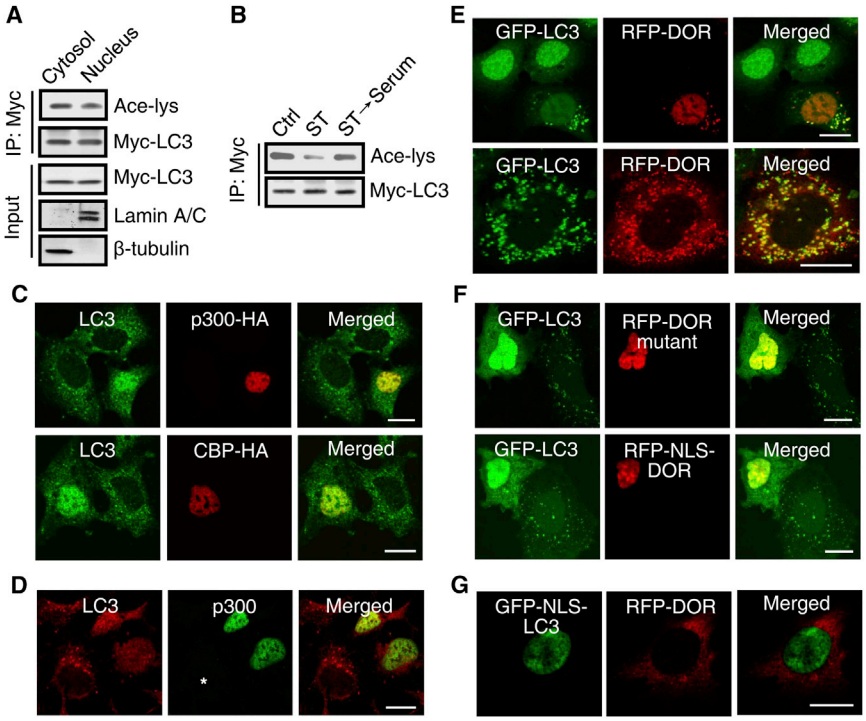

Figure 3. Export of Nuclear LC3 Is Dependent on LC3 Deacetylation and the LC3-Interaction Protein DOR

(A) Cytoplasmic and nuclear Myc-LC3 fractionated from HEK293 cells expressing Myc-LC3 were immunoprecipitated by anti-Myc antibody. Then the immunocomplexes were analyzed with western blot with an anti-acetyl-lysine antibody. Lamin A/C and β-tubulin were used as markers for the nuclear and the cytoplasmic fractions.

(B) Myc-LC3-expressing cells were starved, or were cultured in complete medium for 2 hr after starvation. Then the acetylation of Myc-LC3 was analyzed.

(C) HEK293 cells transiently expressing p300-HA or CBP-HA were starved and stained for LC3 and HA.

(D) HEK293 cells treated with p300 siRNA were fixed and labeled by antibodies against LC3 and p300. *Gene knockdown cell.

(E and F) GFP-LC3 cells were transiently transfected with RFP-DOR (E) or nuclear-fixed RFP-DOR mutant or RFP-NLS-DOR (F). The cells were either untreated or starved and imaged.

(G) HEK293 cells transiently expressing GFP-NLS-LC3 and RFP-DOR were imaged after starvation. Scale bars represent 10 μm. See also Figure S2.

function of nuclear LC3 and its translocation in starvation-induced autophagy. Clearly, knockdown of LC3 raised cellular p62, an indicator of autophagic degradation, and prevented starvation-induced autophagosome/autolysosome formation identified by electron microscopy. Expression of wild-type LC3, but not the NES-LC3 or a nucleus-fixed LC3 containing a nuclear localization signal (NLS-LC3), reversed the effect of LC3 knockdown (Figures 2F–2H). These results indicated a critical role of nuclear pool of LC3 in initiating autophagy.

Export of Nuclear LC3 Is Dependent on LC3 Deacetylation and the LC3-Interaction Protein DOR

We examined whether nuclear LC3 was being modified to a form under starvation conditions where it could specifically participate in autophagosome formation. Protein acetylation is known to play an important role in autophagy (Yi et al., 2012; Lee et al., 2008; Lee and Finkel, 2009; Lin et al., 2012; Füllgrabe et al., 2013; Morselli et al., 2010), and Atg8 (the yeast homolog of LC3) has been shown to be deacetylated in response to starvation (Lee et al., 2008; Lee and Finkel, 2009). Given this, we examined the acetylation status of intracellular LC3 (either endogenous or exogenous Myc-tagged LC3) and its relationship to the export of nuclear LC3. Under nutrient-rich conditions, both nuclear and cytoplasmic forms of LC3-I were acetylated (Figures 3A and S2A). However, cell starvation caused a clear deacetylation of cellular Myc-LC3 that was restored by serum (Figure 3B). Cell starvation-induced deacetylation was also observed in other Atg8 isoforms (Figure S2B). Overexpression of p300 or CBP (CREB-binding protein), two acetyltransferases for Atg8, prevented starvation-induced cytoplasmic redistribution and deacetylation of LC3 (Figures 3C and S2C), whereas p300 RNAi induced such redistribution and led to the formation of cytoplasmic LC3 puncta in nutrient-rich cells (Figures 3D and S2D). These results suggested that modulation of the acetylation-deacetylation cycle of LC3 profoundly affects the subcellular distribution of LC3, with cytoplasmic redistribution of LC3 dependent on LC3 deacetylation. A possible dependence of nuclear export of LC3 on its leucine-rich and chromosomal maintenance region 1 (CRM1)-binding NES (Drake et al., 2010) was excluded, because treatment with CRM1 inhibitor leptomycin B (LMB) had no effect on starvation-induced nuclear export of LC3 (Figure S2E).

The diabetes- and obesity-regulated nuclear factor DOR interacts with LC3, exits the nucleus, and targets to autophagosomes through an mechanistic target of rapamycin (mTOR)- and PI3K III-regulated pathway during autophagy (Mauvezin et al., 2010).

(D) HEK293 cells transiently expression of GFP-NES-LC3 (green) or Cherry-LC3 (red) were starved and imaged.

(E) Representative images of starved cells expressing GFP-NES-LC3 and RFP-DFCP1.

(F) GFP-LC3, GFP-NES-LC3, or GFP-NLS-LC3 was transfected in HeLa cells with either nontargeting siRNA or a pool of LC3 siRNAs (A, B, and C isoforms). After starvation, the cellular p62 level was analyzed with western blot.

(G) Autophagic vacuoles in cells treated as in (F), except that CQ was added in starvation medium, were observed with transmission electron microscopy. The arrows indicate the formed autophagosomes and autolysosomes. Scale bars represent 0.5 μm.

(H) Statistical analysis of cytoplasmic occupancy of autophagic vacuoles in the cells shown in (G).

Data are presented as mean ± SEM, n = 20. ***$p < 0.001$. (A–E) Scale bars represent 5 μm.

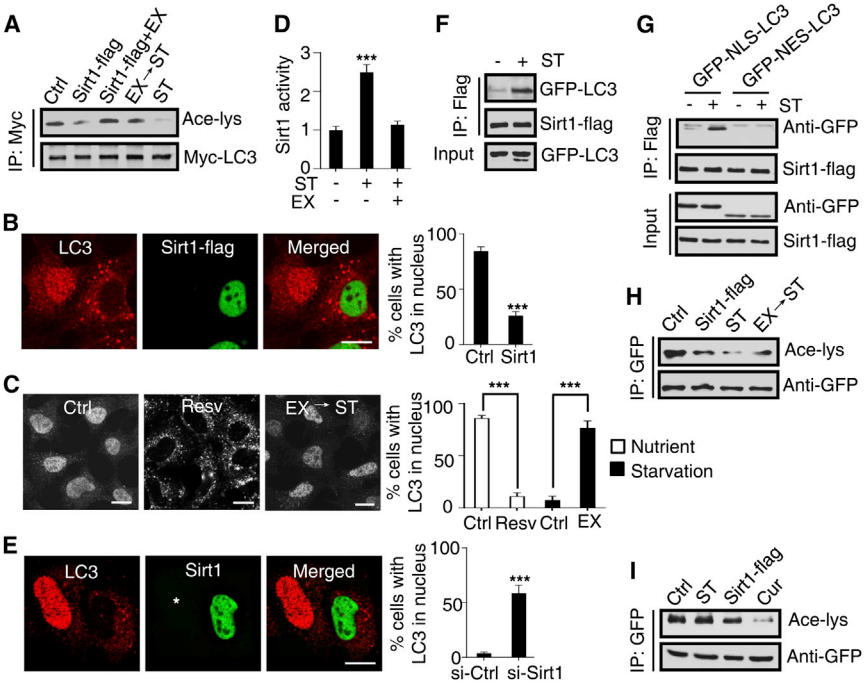

Figure 4. Deacetylation of LC3 in the Nucleus by Sirt1 Is Required for Nuclear Export of LC3

(A) Acetylation of Myc-LC3 in cells overexpression of Sirt1-flag with or without addition of Sirt1 inhibitor EX-527 (EX) detected with immunoprecipitation with an anti-Myc antibody followed by western blot with an anti-acetyl-lysine antibody.

(B) Localization of LC3 in cells overexpressing Sirt1-flag.

(C) HEK293 cells treated with resveratrol (Resv), or starved after EX-527 treatment were fixed and stained for endogenous LC3.

(D) Sirt1-flag was immunoprecipitated from starved cells with or without EX-527, and its activity was quantified using a fluorophore-conjugated acetylated p53 peptide.

(E) Localization of LC3 in starved cells with Sirt1 RNAi. *Sirt1 knockdown cell.

(F and G) Coimmunoprecipitation of Sirt1-flag with GFP-LC3 (F) or GFP-NLS-LC3 (G), but not GFP-NES-LC3 (G), in cells coexpressing Sirt1-flag and each of the LC3s.

(H) Acetylation of GFP-NLS-LC3 either cotransfected with Sirt1-flag, or starved with or without EX-527 pretreatment.

(I) Acetylation of GFP-NES-LC3 in HEK293 cells either cotransfected with Sirt1-flag or starved, or treated with curcumin (Cur). Curcumin was used here as an inhibitor of p300.

The statistical results are shown as means ± SEM (n = 6). ***$p < 0.001$. Scale bars represent 10 μm. See also Figures S3 and S4.

We therefore speculated that DOR contributes to the nuclear export of LC3 under cell starvation. RFP-tagged DOR was transfected into HEK293 cells stably expressing GFP-LC3. Whereas most of the overexpressed RFP-DOR was in the nucleus, some was in the cytoplasm presenting as punctate structures. In these cells, GFP-LC3 showed an increased cytoplasmic distribution and colocalization with the RFP-DOR puncta (Figure 3E, upper images). In addition, upon starvation, most of the nuclear RFP-DOR shifted to the cytoplasm accompanied by enhanced nuclear export of GFP-LC3 (Figure 3E, lower images). Same as that of LC3, this shifting of DOR was independent of CRM1-binding and Atg5 or Atg7 activity (Figure S2F). These results are consistent with previous data (Mauvezin et al., 2010) and imply a synchronous departure of the two proteins from the nucleus. We then used a DOR mutant in which the NES motif is deleted and fails to leave the nucleus (Mauvezin et al., 2010). In cells coexpressing this RFP-DOR mutant, GFP-LC3 was fixed with the RFP-DOR mutant in the nucleus during starvation (Figure 3F). Consistently, in starved cells, the expression of a nucleus-locked RFP-NLS-DOR also localized GFP-LC3 to the nucleus (Figure 3F), whereas the starvation-induced nuclear export of RFP-DOR was unaffected by expression of a nucleus-fixed GFP-NLS-LC3 (Figure 3G). These results suggested that DOR mediates the autophagic export of nuclear LC3.

Deacetylation of LC3 in the Nucleus by Sirt1 Is Required for Nuclear Export of LC3

We next focused on the molecular mechanism of LC3 deacetylation and its role in driving the nucleus-to-cytoplasm redistribution of LC3 and subsequent autophagosome biogenesis. A role of class I/II histone deacetylases (HDACs) was ruled out because treatment of cells with trichostatin A (TSA), a specific inhibitor of class I/II HDACs, neither inhibited the starvation-induced deacetylation nor the nuclear export of LC3 (Figures S3A and S3B). We then tested Sirt1, a member of the sirtuin family of class III histone deacetylases that localizes primarily in the nucleus (Michishita et al., 2005). Previous work has shown that Sirt1 can cause Atg8 deacetylation and that Sirt1 overexpression can stimulate autophagosome formation (Lee et al., 2008). Supporting this, we found that Sirt1 overexpression resulted in LC3 deacetylation, which could be prevented by a specific Sirt1 inhibitor EX-527 (Figure 4A). Notably, overexpression of Sirt1 or treatment with resveratrol (Resv), a Sirt1 activator, led to LC3 redistributing into the cytoplasm and the formation of LC3 puncta, while EX-527 addition prevented starvation-induced nuclear to cytoplasmic redistribution of LC3 (Figures 4B and 4C). Moreover, we clearly detected an increased Sirt1 activity in starved cells (Figure 4D), and RNAi of Sirt1 but not Sirt6 or Sirt7, two other nucleus-localized sirtuins, inhibited starvation-induced nuclear-to-cytoplasmic redistribution and deacetylation of LC3 (Figures 4E and S3C–S3E). Interestingly, p300 RNAi failed to prevent starvation-induced deacetylation of LC3, although it reduced LC3 acetylation in nutrient-rich cells (Figures S3D and S3E). These results suggested that deacetylation of LC3 by Sirt1 is necessary for LC3 to shift its distribution from the nucleus to cytoplasm during cell starvation.

Prolonged oxidative stimuli may lead nuclear Sirt1 to the cytoplasm (Jin et al., 2007). However, in our study, either

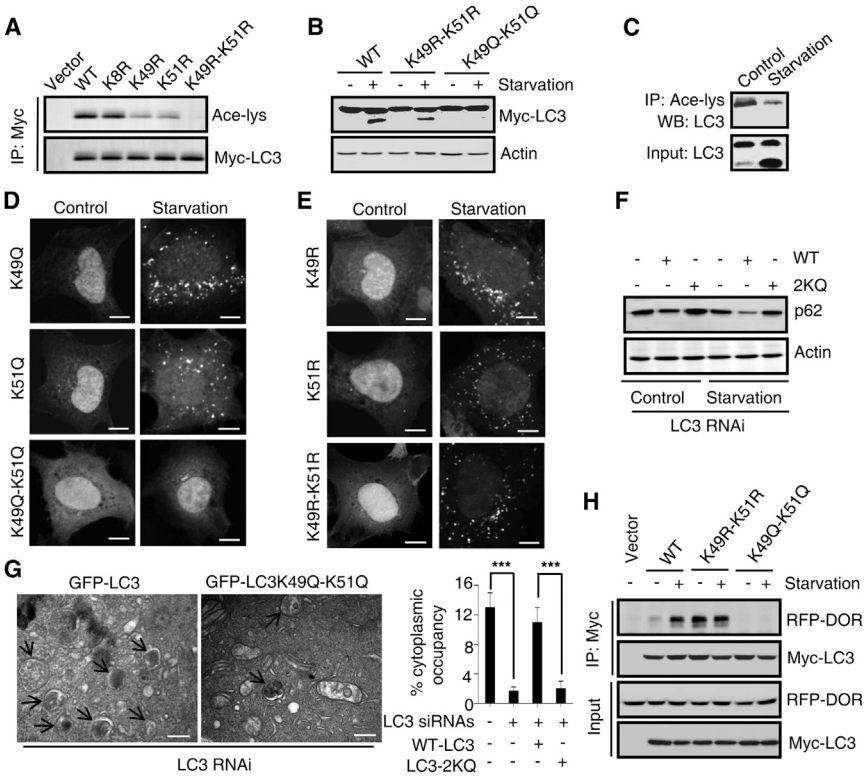

Figure 5. K49 and K51 Are the Main Acetylation Sites of LC3

(A) HEK293 cells were transfected with Myc-tagged wild-type LC3 (WT) or each of the LC3 mutants. The exogenous LC3 or each of the LC3 mutants was immunoprecipitated with anti-Myc and analyzed with western blot for acetyl-lysine.

(B) HEK293 cells transfected with Myc-tagged LC3 or the LC3 mutants were starved, then the cells were analyzed with western blot using an anti-Myc antibody. Note the formation of Myc-LC3-PE.

(C) HEK293 cells with or without starvation were analyzed for LC3 acetylation with immunoprecipitation and western blot using anti-acetyl-lysine and anti-LC3 antibodies, respectively.

(D and E) Distributions of GFP-tagged LC3 mutants in cells with or without starvation. Scale bars represent 5 μm.

(F) HeLa cells with LC3 RNAi were transfected with GFP-LC3 or GFP-LC3K49Q-K51Q (2KQ) and were starved. The lysates were analyzed with western blot with a p62 antibody. (G) GFP-LC3 or GFP-LC3K49Q-K51Q was transfected in HeLa cells with a pool of LC3 siRNAs (A, B, and C isoforms). The cells were starved with CQ and observed with transmission electron microscopy. The arrows indicate the autophagic vacuoles including autophagosomes and autolysosomes. The quantification of cytoplasmic occupancy of autophagic vacuoles in the cells is shown. Data are presented as mean ± SEM, n = 20. ***$p < 0.001$. Scale bars represent 0.5 μm.

(H) HEK293 cells transiently transfected with RFP-DOR and Myc-tagged wild-type LC3 (WT) or each of the LC3 mutants were starved. Then the cell lysates were immunoprecipitated with anti-Myc antibody, and the immunocomplexes were subjected to western blot with anti-RFP antibody.

See also Figure S5.

endogenous or the exogenous Sirt1 stayed in the nucleus during cell starvation (Figures S4A and S4B), suggesting LC3 deacetylation by Sirt1 occurs in the nucleus. Indeed, we found, by coimmunoprecipitation, cell starvation induced interaction of Sirt1-flag with GFP-LC3 or GFP-NLS-LC3, the nucleus-localized GFP-LC3, but not with GFP-NES-LC3 that predominantly localized in the cytoplasm (Figures 4F and 4G). Consistently, in response to Sirt1 overexpression or cell starvation, GFP-NLS-LC3, but not GFP-NES-LC3, was deacetylated (Figures 4H and 4I). Thus, deacetylation of LC3 in the nucleus by Sirt1 is required for the export of nuclear LC3.

K49 and K51 Sites Are the Main Acetylation Sites of LC3

LC3 carries eight lysine residues, among which Lys8, Lys49, and Lys51 are species-conserved. To identify the acetylation site(s) of LC3, LC3 mutants were constructed in which each of the eight lysine residues was changed to arginine via site-directed mutagenesis. Myc-tagged LC3-KR mutants were transfected into HEK293 cells and assessed for their acetylation. This revealed that lysine-to-arginine replacement at Lys49 or Lys51 reduces LC3 acetylation, and double replacement at the positions completely abolishes LC3 acetylation (Figure 5A); therefore, Lys49 and Lys51 are the major acetylation sites on LC3, and they were confirmed by mass spectrometry (Figure S5A). Consistently, upon cell starvation, we detected PE-conjugated LC3 and LC3K49R-K51R (Figure 5B), but not PE-conjugated LC3K49Q-K51Q, a LC3 mutant in which the lysines at Lys49 and Lys51 were replaced by glutamine, mimicking the acetylated LC3 (Choudhary et al., 2009). In addition, GFP-LC3K49Q-K51Q failed to be cleaved to generate the free GFP fragment (Figure S5B). Furthermore, we found that acetylation was predominant in LC3-I rather than LC3-II (Figure 5C). These data suggested that acetylation of LC3 at Lys49 and Lys51 prevents LC3 from PE conjugation. Morphologically, both the acetylated and deacetylated LC3 mutants showed a nuclear and cytoplasmic distribution similar to that of wild-type LC3. Upon cell starvation, all the LC3 mutants except LC3K49Q-K51Q formed puncta in the cytoplasm, accompanied by the redistribution of the proteins out of the nucleus (Figures 5D, 5E, and S5C), indicating a requirement of deacetylation at Lys49 or Lys51 for LC3 to shift its distribution onto autophagic membranes in the cytoplasm. Because steady-state pools of LC3K49R-K51R were still enriched in the nucleus in nutrient-rich cells, deacetylation of LC3 alone is not sufficient to induce its cytoplasmic redistribution in the absence of other autophagy inducers. Finally, we checked the restoration of LC3 RNAi-induced accumulation of p62 and inhibition of autophagosome formation by LC3K49Q-K51Q. As expected, only the expression of wild-type of LC3, but not LC3K49Q-K51Q, reversed the effect of LC3 RNAi on p62 degradation and autophagosome/autolysosome formation (Figures 5F and 5G), suggesting an essential role of deacetylation at the sites in starvation-triggered autophagy.

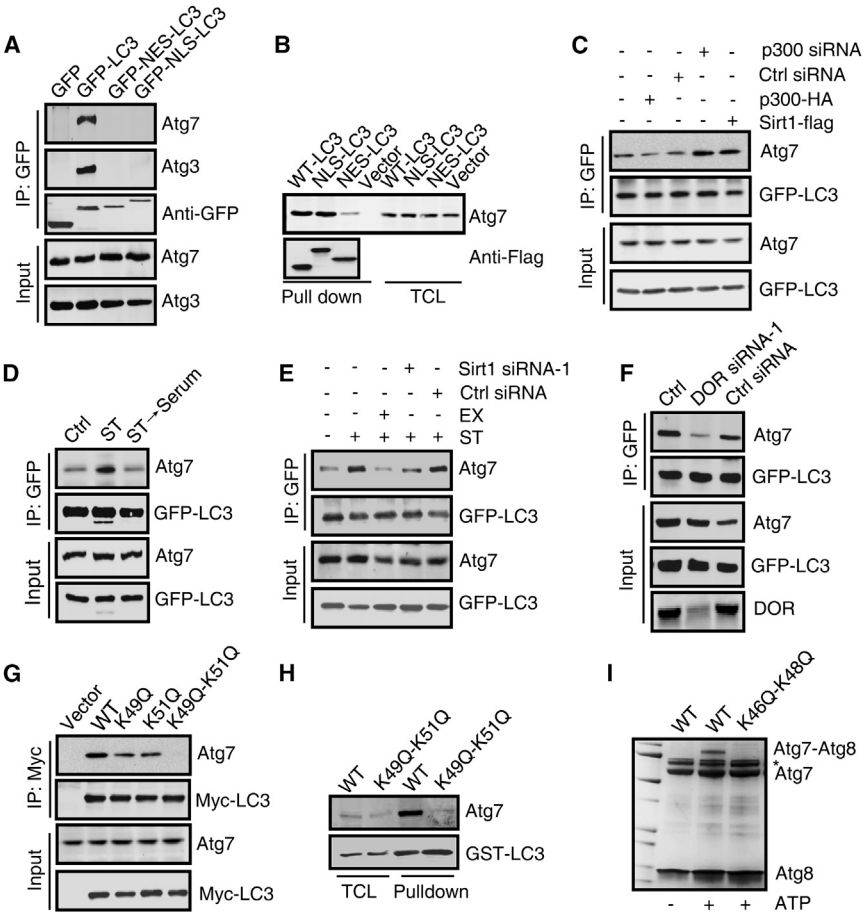

Figure 6. Deacetylation of LC3 Is Essential for LC3-Atg7 Interaction

(A) Interaction of endogenous Atg7 and Atg3 with GFP-LC3, GFP-NES-LC3, or GFP-NLS-LC3 in transfected HEK293 cells by immunoprecipitation with a GFP antibody followed by western blot with anti-Atg7 or anti-Atg3 antibody.

(B) Flag-LC3, Flag-NLS-LC3, and Flag-NES-LC3 proteins were purified from HEK293 cells expressing each of the plasmids. Then each of the purified proteins was incubated with lysate of HeLa cells, and a pull-down assay for Atg7 was performed using specific Atg7 and Flag antibodies. TCL, total cell lysates.

(C) GFP-LC3-expressing cells were either transfected with p300-HA or p300 siRNAs or Sirt1-flag, then the coimmunoprecipitation of endogenous Atg7 with GFP-LC3 was analyzed.

(D) GFP-LC3 cells were starved or recultured in replete growth medium for 2 hr after starvation. Then the coimmunoprecipitation of endogenous Atg7 with GFP-LC3 was analyzed.

(E and F) The coimmunoprecipitation of endogenous Atg7 with GFP-LC3 was analyzed in GFP-LC3 cells starved with or without the addition of EX-527 or Sirt1 siRNA (E) or DOR siRNA (F).

(G) Coimmunoprecipitation of Atg7 with indicated Myc-LC3s in transfected cells.

(H) HEK293 cell lysates were incubated with bacterially expressed and purified GST-LC3^{G120} or GST-LC3^{G120}-K49Q-K51Q, and bound Atg7 was detected with anti-Atg7 antibody. TCL, total cell lysates.

(I) In vitro binding assay of Atg7 with Atg8^{G116} or Atg7 with Atg8^{G116}-K46Q-K48Q. *Nonspecific bands.

See also Figure S6.

We further examined the interaction between DOR and the LC3 mutants in cells expressing each of the Myc-tagged LC3 mutants and RFP-DOR. When a weak association of Myc-LC3 with RFP-DOR was detected in cells at nutrient conditions that may reflect the requirement for basal autophagy, cell starvation dramatically enhanced the association (Figure 5H). Interestingly, at both basal and starvation conditions, whereas a strong coimmunoprecipitation of RFP-DOR with Myc-LC3K49R-K51R was revealed, no detectable RFP-DOR was coimmunoprecipitated by Myc-LC3K49Q-K51Q (Figure 5H), indicating a specific interaction of DOR with deacetylated LC3.

Deacetylation of LC3 Is Essential for LC3-Atg7 Interaction

Conjugation of LC3 to PE requires LC3 to interact sequentially with Atg7 and Atg3 (Ichimura et al., 2000; Nakatogawa et al., 2007). To investigate the mechanism by which only deacetylated LC3 undergoes lipidation and membrane association, we examined the interaction between LC3 and Atg7. When expressed in nutrient-rich cells, neither GFP-NES-LC3 nor GFP-NLS-LC3 coimmunoprecipitated Atg7 or Atg3, in contrast to GFP-LC3 (Figure 6A). In addition, purified Flag-LC3 and Flag-NLS-LC3 but not Flag-NES-LC3, pulled down Atg7 from the cell lysates (Figure 6B). These results suggested that normal nucleocytoplasmic exchange of LC3 in cell is required for LC3 to interact with Atg7. The coimmunoprecipitation of Atg7 with GFP-LC3 was controlled by LC3 deacetylation because it was suppressed by p300 overexpression and augmented by p300 RNAi or Sirt1 overexpression (Figure 6C). We then analyzed LC3-Atg7 interaction in starved cells. Starvation markedly enhanced the coimmunoprecipitation of Atg7 with GFP-LC3, and this enhancement was inhibited by serum addition (Figure 6D). Starvation-induced LC3-Atg7 interactions were suppressed by EX-527 or Sirt1 RNAi, suggesting they were dependent on Sirt1 activity (Figures 6E and S6A). Furthermore, knockdown of DOR dramatically diminished the starvation-induced association of GFP-LC3 with Atg7, demonstrating a role of DOR in mediating the interaction (Figures 6F and S6B). Together, these results suggest that by controlling LC3 deacetylation in the nucleus and its subsequent redistribution, Sirt1 regulates LC3-Atg7 interactions during cell starvation.

We further determined the interaction between Atg7 and the acetylation-fixed LC3 mutants. In cells expressing each of the LC3 mutants, change of lysine to glutamine at Lys49 or Lys51 significantly inactivated LC3 for association with Atg7 (Figure 6G). In addition, purified recombinant GST-LC3^{G120}, but not GST-LC3^{G120}K49Q-K51Q, pulled down Atg7 from the cell lysates (Figure 6H). Furthermore, in vitro Atg7-Atg8 binding assays using recombinant yeast Atg7 and Atg8^{G116} indicated that incubation of Atg7 with Agt8^{G116}, but not Atg8^{G116}K46Q-K48Q (K49

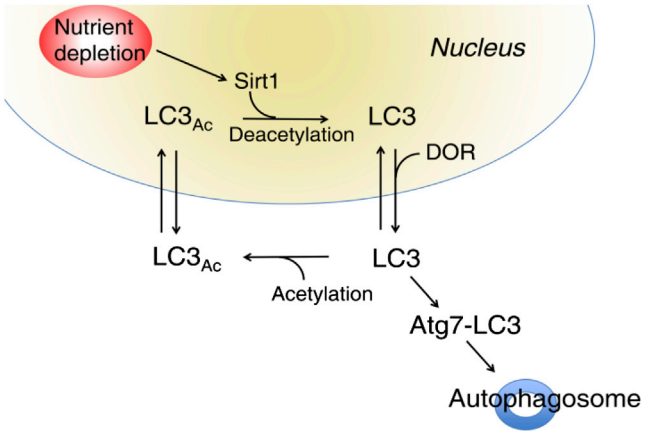

Figure 7. Schematic Model for Deacetylation and Translocation of Nuclear LC3 in Starvation-Induced Autophagy

In response to nutrient depletion, activated Sirt1 interacts with and deacetylates nuclear LC3. Through binding to DOR, deacetylated LC3 is transported to the cytoplasm to carry out PE conjugation by sequential interaction with Atg7 and Atg3.

and K51 in LC3), led to the formation of an Atg7-Atg8 thioester bond (Figure 6I). Together, these data suggest that deacetylation of LC3 at Lys49 and Lys51 is essential for LC3 to bind Atg7.

DISCUSSION

The existence of substantial amounts of LC3 in the nucleus has been recognized for a long time, but its significance in autophagy has not been appreciated because it is generally acknowledged that the cytosolic localization of LC3 is a prerequisite for this protein to play a prominent role in autophagy. In this study, we identified an autophagic signal-controlled acetylation/deacetylation-dependent nucleocytoplasmic transport mechanism for LC3 that is essential for autophagosome formation (Figure 7). During starvation, nuclear-localized Sirt1 becomes activated and deacetylates LC3 in the nucleus. Once the deacetylated molecules shift into the cytoplasm, they now interact with autophagic effectors including Atg7, and initiate autophagy. When nutrients are resupplied, reacetylation of LC3 prevents it from interacting with Atg7 and other autophagy effectors. Consequently, LC3 reestablishes its prior nuclear enrichment. An important feature of this model is that LC3 shuttling allows its abundance in the nucleus and cytoplasm to be regulated. This is likely important for controlling the timing and initiation of autophagy in response to starvation. Specifically, by having a high concentration of LC3 in the nucleus (where Sirt1 is localized) at the time starvation is initiated, LC3 can become quickly and efficiently deacetylated to facilitate autophagosome biogenesis once it moves into the cytoplasm.

Given that Sirt1 activity is required for autophagy and is capable of deacetylating Atg5, Atg7, and Atg8 under cell starvation, whether the deacetylation events of these proteins are required and how they contribute to autophagy remain unknown. Our data showing a temporal-spatial control of LC3 activity by Sirt1 in autophagosome formation provide a mechanism for a direct involvement of Sirt1 in autophagic machinery modulation. Although the function of Atg5 and Atg7 deacetylation in autophagy needs to be elucidated, by combining the requirement of acetylation of Atg3 in *Saccharomyces cerevisiae* and of ULK1 in mammalian cells, it is likely that this acetylation/deacetylation of protein modification is widely used by eukaryotic cells to govern the well-conserved cell degradation process. Clarification of the role of each of these acetylation/deacetylation events may need further identification of specific acetyltransferases or deacetylases for individual Atgs. In addition, cell starvation can evoke multiple cell signaling events including the activation of AMPK and inactivation of mTOR. How theses signaling events influence Sirt1 activity, especially the link between Sirt1 activation and mTOR inactivation, a general mediator for nonselective autophagy, need to be elucidated in future. As an LC3-interaction protein, DOR is proposed to contribute to autophagy in a LC3-interaction-independent or -dependent mechanism (Nowak et al., 2009). Of the two, the latter involves an interaction of DOR and LC3 in the cytoplasm and a recruitment of DOR-associated LC3 to the autophagosome membranes. We identified here that DOR-LC3 occurs initially in the nucleus during autophagy. Through specific interaction with deacetylated LC3 in the nucleus, mediation of the export of LC3 from the nucleus is the primary role of DOR in autophagy. Different from the report showing a requirement of Atg5 for the nuclear export of DOR (Nowak et al., 2009), we found that DOR clearly redistributed from the nucleus to the cytoplasm in starved *Atg5*$^{-/-}$ or *Atg7*$^{-/-}$ cells like that of LC3, indicating an independence from Atg5 and Atg7 activities. This suggests that DOR-mediated LC3 translocation is an early event of autophagy initiated by Sirt1 activation rather than downstream of Atg12-Atg5 or Atg7-LC3 step.

We found that under replete growth conditions, both the nuclear and cytoplasmic LC3 are in an acetylated form. In addition to be deacetylated for autophagy, acetylation of LC3 under basal conditions may be required for its functions besides autophagy. It has been reported that soluble LC3 interacts directly with fibronectin mRNA, assisting its translation by ribosomal recruitment (Zhou et al., 1997; Zhou and Rabinovitch, 1998). Nonlipidated LC3-I is selectively involved in the formation of complexes mediating endoplasmic reticulum-associated degradation (Bernasconi et al., 2012) or facilitating virus replication (Reggiori et al., 2010), in an autophagy-independent manner. In addition to the proteolysis in lysosomes, it has recently been demonstrated that LC3 is processed by the 20S proteasome (Gao et al., 2010b), suggesting a possibility that acetylation of LC3 may stabilize the protein under nutrient conditions, preventing its lysosome-independent degradation.

Identification of the K49 and K51 acetylation sites of LC3 helps to not only the confirmation of the effect of Sirt1 on LC3 translocation, but also the determination of the role of deacetylation in Atg7 recognition. Whereas DOR and Atg3 own the Atg8-family interacting motif (AIM), no typical AIM has been identified in Atg7 (Noda et al., 2010). Structural studies

have suggested that the Atg8-Atg7 interaction involves both the hydrophobic residues buried in the hydrophobic pockets of Atg8 and the C-terminal helices of Atg7 (Hong et al., 2011; Noda et al., 2010, 2011). Whereas the Lys51 is located in one of the hydrophobic pockets, the Lys49 is at the connection site of the two pockets, and both are required for the AIM recognition of LC3 (Noda et al., 2010, 2011). In such a scenario, acetylation at these residues may function to interfere with the formation of a hydrophobic binding interface between LC3 and Atg7. Nevertheless, because glutamine is more hydrophobic than lysine, the finding that lysine-to-glutamine replacement prevents the LC3-Atg7 interaction suggests a crucial role of the ionic interactions between the acidic residues in the C-terminal region of Atg7 and the basic residues of LC3, including Lys49, in the LC3-Atg7 interaction (Ichimura et al., 2008; Noda et al., 2011). Acetylation at Lys49 and Lys51 probably disturbs the ionic interactions by neutralizing the positive charge of the lysine side chain. In addition, acetylation not only neutralizes the positive charge of the lysine, but also impairs its ability to form hydrogen bonds. It is known that the formation of a hydrogen bond using Tyr62 in Atg8 is also involved in the Atg7-Atg8 interaction (Hong et al., 2011), so it is possible that acetylation at Lys49 and Lys51 affects the formation of the hydrogen bond through Tyr62 or Lys49 and Lys51 themselves.

EXPERIMENTAL PROCEDURES

Plasmids, Antibodies, and Reagents

Plasmids, antibodies, and reagents are described in the Supplemental Experimental Procedures.

Cell Culture and Transfection

Cells were grown in Dulbecco's modified Eagle's medium supplemented with 10% fetal bovine serum at 37°C under 5% CO_2. Transient transfections were performed using Lipofectamine 2000 according to the manufacturer's instructions (Invitrogen). Cells were analyzed 18–24 hr after transfection. Cells stably expressing GFP-tagged wild-type LC3 or LC3 mutants or Sirt1 were created by transient transfection followed by selection with G418. See the Supplemental Experimental Procedures for details.

Autophagy Induction

To induce autophagy, cells were washed three times with prewarmed PBS then incubated in starvation medium (1% BSA, 140 mM NaCl, 1 mM $CaCl_2$, 1 mM $MgCl_2$, 5 mM glucose, and 20 mM HEPES [pH 7.4]) at 37°C for 1 hr under 5% CO_2.

Fluorescence Microscopy

Images were acquired on a scanning confocal microscope (LSM 510; Carl Zeiss) and analyzed with the LSM 510 software (Carl Zeiss). Photoactivation was performed with high-level (~1 mW) 405 nm laser light through the objective. Photoactivated protein was imaged under low-intensity excitation (~1 μW) of the 488 nm laser. Selective photobleaching was performed using the 488 nm laser at full power. Then the 488 nm laser line was used for excitation. Single-plane images were captured from 1.7 μm optical slices every 20 min for 2 hr. See the Supplemental Experimental Procedures for details.

Electron Microscopy

Electron microscopy was performed as described previously (Ylä-Anttila et al., 2009). Briefly, cells were fixed in 2.5% glutaraldehyde for 4 hr at room temperature, and then postfixed in 1% OsO_4 followed by 2% uranyl acetate. After ethanol and propylene oxide dehydration and embedding in polybed 812 resin (Polysciences, 025950-1), thin sections (80 nm) were poststained with 2% uranyl acetate followed by 0.3% lead citrate. Sample sections were viewed on a TECNAI 10 transmission electron microscope (FEI) at 80 kV. For autophagic vacuole quantification, 20 micrographs, primary magnification 11,500×, were taken with systematic random sampling from each sample. The cytoplasmic volume fraction of autophagic vacuoles was estimated using MetaMorph (Universal Imaging).

Immunoprecipitation and Western Blot

Cells were lysed in lysis buffer and subjected to immunoprecipitation with primary antibody. Immunocomplexes were separated by SDS-PAGE and detected with western blot analyses. For details of conditions and antibodies used, see the Supplemental Experimental Procedures.

In Vitro Assay of Atg7-Atg8 Interaction

Procedures for protein purification are described in the Supplemental Experimental Procedures. To detect Atg8-Atg7 thioester intermediates, 0.4 μM $Atg8^{G116}$ and 0.1 μM Atg7 were incubated in reaction buffer containing 50 mM HEPES (pH 7.0), 150 mM NaCl, 0.2 mM dithiothreitol, 1 mM ATP, and 1 mM $MgCl_2$ at 4°C for 15 min. The incubated mixture was denatured by nonreducing sample buffer, subjected to SDS-PAGE, and then depicted with Coomassie blue staining.

In Vitro Pull-Down Assay

Recombinant proteins that were purified from bacterial or from HEK293 cells were incubated with total cell protein extract at 4°C for 4 hr. Then glutathione sepharose 4B beads or anti-Flag antibody conjugated agarose were added to the mixture, followed by further incubation at 4°C for 2 hr. Immunocomplexes were washed four times with wash buffer (50 mM Tris-HCl, 50 mM NaCl, 0.1% Triton X-100, 10% glycerol, protease inhibitors, 1 mM phenylmethanesulfonylfluoride, and 1 mM dithiothreitol) and subjected to western blot analysis.

Fluorometric Sirt1 Activity Assay

Sirt1-flag was immunoprecipitated from cells transfected with Sirt1-flag. Eluted protein was incubated with 100 μM of NAD^+ and 25 mM fluorescently labeled acetylated p53 peptide for 10 min at 37°C according to the manufacturer's instructions (ENZO). The reaction was stopped with developer solution containing 2 mM nicotinamide to inhibit Sirt1 and protease to digest deacetylated p53 peptide. Sirt1 activity was assessed by measuring the fluorescent emission at 460 nm, following excitation at 360 nm.

High-Performance Liquid Chromatography/Tandem Mass Spectrometry in an LTQ Mass Spectrometer

Purified Flag-LC3 from HEK293 cells was analyzed on NuPAGE Tris-Bis 4%–12% polyacrylamide gradient gels run in 1× Mops buffer, and depicted with colloidal Coomassie blue staining. Bands were excised, digested with trypsin, and analyzed with an LTQ-Orbitrap mass spectrometer at the Center of Biomedical Analysis, Tsinghua University.

SUPPLEMENTAL INFORMATION

Supplemental Information includes Supplemental Experimental Procedures and six figures and can be found with this article online at http://dx.doi.org/10.1016/j.molcel.2014.12.013.

AUTHOR CONTRIBUTIONS

W.L. and R.H. designed the experiments. R.H., Y.X., W.W., X.S., J.Q., and Z.Y. performed the experiments. W.L. and J.L.-S. wrote the manuscript. All authors discussed the results and commented on the manuscript.

ACKNOWLEDGMENTS

We are grateful to the Imaging Center of Zhejiang University School of Medicine for their assistance in confocal microscopy and electron microscopy.

We thank Hong Liu, Tingting Song (Zhejiang University), and Jingjing Tong (Tsinghua University) for other technical support and members of Dr. Liu's lab for helpful discussions. This study was supported by the National Basic Research Program of China (2011CB910100 and 2013CB910200) and National Natural Science Foundation of China (31171288 and 31271431).

Received: August 14, 2014
Revised: October 30, 2014
Accepted: December 5, 2014
Published: January 15, 2015

REFERENCES

Axe, E.L., Walker, S.A., Manifava, M., Chandra, P., Roderick, H.L., Habermann, A., Griffiths, G., and Ktistakis, N.T. (2008). Autophagosome formation from membrane compartments enriched in phosphatidylinositol 3-phosphate and dynamically connected to the endoplasmic reticulum. J. Cell Biol. *182*, 685–701.

Bernasconi, R., Galli, C., Noack, J., Bianchi, S., de Haan, C.A., Reggiori, F., and Molinari, M. (2012). Role of the SEL1L:LC3-I complex as an ERAD tuning receptor in the mammalian ER. Mol. Cell *46*, 809–819.

Choudhary, C., Kumar, C., Gnad, F., Nielsen, M.L., Rehman, M., Walther, T.C., Olsen, J.V., and Mann, M. (2009). Lysine acetylation targets protein complexes and co-regulates major cellular functions. Science *325*, 834–840.

Drake, K.R., Kang, M., and Kenworthy, A.K. (2010). Nucleocytoplasmic distribution and dynamics of the autophagosome marker EGFP-LC3. PLoS ONE *5*, e9806.

Eskelinen, E.L. (2008). New insights into the mechanisms of macroautophagy in mammalian cells. Int Rev Cell Mol Biol *266*, 207–247.

Füllgrabe, J., Lynch-Day, M.A., Heldring, N., Li, W., Struijk, R.B., Ma, Q., Hermanson, O., Rosenfeld, M.G., Klionsky, D.J., and Joseph, B. (2013). The histone H4 lysine 16 acetyltransferase hMOF regulates the outcome of autophagy. Nature *500*, 468–471.

Furuta, S., Miura, K., Copeland, T., Shang, W.H., Oshima, A., and Kamata, T. (2002). Light Chain 3 associates with a Sos1 guanine nucleotide exchange factor: its significance in the Sos1-mediated Rac1 signaling leading to membrane ruffling. Oncogene *21*, 7060–7066.

Gao, W., Kang, J.H., Liao, Y., Ding, W.X., Gambotto, A.A., Watkins, S.C., Liu, Y.J., Stolz, D.B., and Yin, X.M. (2010a). Biochemical isolation and characterization of the tubulovesicular LC3-positive autophagosomal compartment. J. Biol. Chem. *285*, 1371–1383.

Gao, Z., Gammoh, N., Wong, P.M., Erdjument-Bromage, H., Tempst, P., and Jiang, X. (2010b). Processing of autophagic protein LC3 by the 20S proteasome. Autophagy *6*, 126–137.

Guo, Y., Chang, C., Huang, R., Liu, B., Bao, L., and Liu, W. (2012). AP1 is essential for generation of autophagosomes from the trans-Golgi network. J. Cell Sci. *125*, 1706–1715.

Hailey, D.W., Rambold, A.S., Satpute-Krishnan, P., Mitra, K., Sougrat, R., Kim, P.K., and Lippincott-Schwartz, J. (2010). Mitochondria supply membranes for autophagosome biogenesis during starvation. Cell *141*, 656–667.

Hong, S.B., Kim, B.W., Lee, K.E., Kim, S.W., Jeon, H., Kim, J., and Song, H.K. (2011). Insights into noncanonical E1 enzyme activation from the structure of autophagic E1 Atg7 with Atg8. Nat. Struct. Mol. Biol. *18*, 1323–1330.

Ichimura, Y., Kirisako, T., Takao, T., Satomi, Y., Shimonishi, Y., Ishihara, N., Mizushima, N., Tanida, I., Kominami, E., Ohsumi, M., et al. (2000). A ubiquitin-like system mediates protein lipidation. Nature *408*, 488–492.

Ichimura, Y., Kumanomidou, T., Sou, Y.S., Mizushima, T., Ezaki, J., Ueno, T., Kominami, E., Yamane, T., Tanaka, K., and Komatsu, M. (2008). Structural basis for sorting mechanism of p62 in selective autophagy. J. Biol. Chem. *283*, 22847–22857.

Jin, Q., Yan, T., Ge, X., Sun, C., Shi, X., and Zhai, Q. (2007). Cytoplasm-localized SIRT1 enhances apoptosis. J. Cell. Physiol. *213*, 88–97.

Kamada, Y., Funakoshi, T., Shintani, T., Nagano, K., Ohsumi, M., and Ohsumi, Y. (2000). Tor-mediated induction of autophagy via an Apg1 protein kinase complex. J. Cell Biol. *150*, 1507–1513.

Kim, J., Kundu, M., Viollet, B., and Guan, K.L. (2011). AMPK and mTOR regulate autophagy through direct phosphorylation of Ulk1. Nat. Cell Biol. *13*, 132–141.

Klionsky, D.J. (2007). Autophagy: from phenomenology to molecular understanding in less than a decade. Nat. Rev. Mol. Cell Biol. *8*, 931–937.

Kraft, L.J., Nguyen, T.A., Vogel, S.S., and Kenworthy, A.K. (2014). Size, stoichiometry, and organization of soluble LC3-associated complexes. Autophagy *10*, 861–877.

Lee, I.H., and Finkel, T. (2009). Regulation of autophagy by the p300 acetyltransferase. J. Biol. Chem. *284*, 6322–6328.

Lee, I.H., Cao, L., Mostoslavsky, R., Lombard, D.B., Liu, J., Bruns, N.E., Tsokos, M., Alt, F.W., and Finkel, T. (2008). A role for the NAD-dependent deacetylase Sirt1 in the regulation of autophagy. Proc. Natl. Acad. Sci. USA *105*, 3374–3379.

Lin, S.Y., Li, T.Y., Liu, Q., Zhang, C., Li, X., Chen, Y., Zhang, S.M., Lian, G., Liu, Q., Ruan, K., et al. (2012). GSK3-TIP60-ULK1 signaling pathway links growth factor deprivation to autophagy. Science *336*, 477–481.

Matsunaga, K., Morita, E., Saitoh, T., Akira, S., Ktistakis, N.T., Izumi, T., Noda, T., and Yoshimori, T. (2010). Autophagy requires endoplasmic reticulum targeting of the PI3-kinase complex via Atg14L. J. Cell Biol. *190*, 511–521.

Mauvezin, C., Orpinell, M., Francis, V.A., Mansilla, F., Duran, J., Ribas, V., Palacín, M., Boya, P., Teleman, A.A., and Zorzano, A. (2010). The nuclear cofactor DOR regulates autophagy in mammalian and Drosophila cells. EMBO Rep. *11*, 37–44.

Michishita, E., Park, J.Y., Burneskis, J.M., Barrett, J.C., and Horikawa, I. (2005). Evolutionarily conserved and nonconserved cellular localizations and functions of human SIRT proteins. Mol. Biol. Cell *16*, 4623–4635.

Mizushima, N. (2007). Autophagy: process and function. Genes Dev. *21*, 2861–2873.

Mizushima, N., Yoshimori, T., and Levine, B. (2010). Methods in mammalian autophagy research. Cell *140*, 313–326.

Morselli, E., Maiuri, M.C., Markaki, M., Megalou, E., Pasparaki, A., Palikaras, K., Criollo, A., Galluzzi, L., Malik, S.A., Vitale, I., et al. (2010). Caloric restriction and resveratrol promote longevity through the Sirtuin-1-dependent induction of autophagy. Cell Death Dis. *1*, e10.

Nakatogawa, H., Ichimura, Y., and Ohsumi, Y. (2007). Atg8, a ubiquitin-like protein required for autophagosome formation, mediates membrane tethering and hemifusion. Cell *130*, 165–178.

Noda, N.N., Ohsumi, Y., and Inagaki, F. (2010). Atg8-family interacting motif crucial for selective autophagy. FEBS Lett. *584*, 1379–1385.

Noda, N.N., Satoo, K., Fujioka, Y., Kumeta, H., Ogura, K., Nakatogawa, H., Ohsumi, Y., and Inagaki, F. (2011). Structural basis of Atg8 activation by a homodimeric E1, Atg7. Mol. Cell *44*, 462–475.

Nowak, J., Archange, C., Tardivel-Lacombe, J., Pontarotti, P., Pébusque, M.J., Vaccaro, M.I., Velasco, G., Dagorn, J.C., and Iovanna, J.L. (2009). The TP53INP2 protein is required for autophagy in mammalian cells. Mol. Biol. Cell *20*, 870–881.

Pankiv, S., Alemu, E.A., Brech, A., Bruun, J.A., Lamark, T., Overvatn, A., Bjørkøy, G., and Johansen, T. (2010). FYCO1 is a Rab7 effector that binds to LC3 and PI3P to mediate microtubule plus end-directed vesicle transport. J. Cell Biol. *188*, 253–269.

Reggiori, F., Monastyrska, I., Verheije, M.H., Calì, T., Ulasli, M., Bianchi, S., Bernasconi, R., de Haan, C.A., and Molinari, M. (2010). Coronaviruses Hijack the LC3-I-positive EDEMosomes, ER-derived vesicles exporting short-lived ERAD regulators, for replication. Cell Host Microbe *7*, 500–508.

Tang, D., Kang, R., Livesey, K.M., Cheh, C.W., Farkas, A., Loughran, P., Hoppe, G., Bianchi, M.E., Tracey, K.J., Zeh, H.J., 3rd, and Lotze, M.T. (2010). Endogenous HMGB1 regulates autophagy. J. Cell Biol. *190*, 881–892.

Waters, S., Marchbank, K., Solomon, E., Whitehouse, C., and Gautel, M. (2009). Interactions with LC3 and polyubiquitin chains link nbr1 to autophagic protein turnover. FEBS Lett. *583*, 1846–1852.

Wei, Y., Zou, Z., Becker, N., Anderson, M., Sumpter, R., Xiao, G., Kinch, L., Koduru, P., Christudass, C.S., Veltri, R.W., et al. (2013). EGFR-mediated Beclin 1 phosphorylation in autophagy suppression, tumor progression, and tumor chemoresistance. Cell *154*, 1269–1284.

Yi, C., Ma, M., Ran, L., Zheng, J., Tong, J., Zhu, J., Ma, C., Sun, Y., Zhang, S., Feng, W., et al. (2012). Function and molecular mechanism of acetylation in autophagy regulation. Science *336*, 474–477.

Ylä-Anttila, P., Vihinen, H., Jokitalo, E., and Eskelinen, E.L. (2009). Monitoring autophagy by electron microscopy in Mammalian cells. Methods Enzymol. *452*, 143–164.

Zhou, B., and Rabinovitch, M. (1998). Microtubule involvement in translational regulation of fibronectin expression by light chain 3 of microtubule-associated protein 1 in vascular smooth muscle cells. Circ. Res. *83*, 481–489.

Zhou, B., Boudreau, N., Coulber, C., Hammarback, J., and Rabinovitch, M. (1997). Microtubule-associated protein 1 light chain 3 is a fibronectin mRNA-binding protein linked to mRNA translation in lamb vascular smooth muscle cells. J. Clin. Invest. *100*, 3070–3082.